International Conference on Adaptive Modeling and Simulation
ADMOS 2023
F.Larsson and P.Díez

THE USE OF ADAPTIVE FEM-SPH TECHNIQUE IN HIGH-VELOCITY IMPACT SIMULATIONS

ALEKSANDR CHERNIAEV*

* Department of Mechanical, Automotive and Materials Engineering, University of Windsor,
401 Sunset Ave., Windsor, Ontario, Canada N9B 3P4
e-mail: aleksandr.cherniaev@uwindsor.ca, web page: www.uwindsor.ca/engineering/mame/cherniaev

Key words: High Velocity Impact, Adaptive FEM-SPH Modeling, Aerospace Engineering

1 INTRODUCTION

It is well known that while the meshless smoothed particles hydrodynamics (SPH) technique is often advantageous in modelling scenarios involving extreme deformations and fragmentation, the finite element method (FEM) in its Lagrangian implementation is well-suited for tracking the materials' interfaces. To use the advantages of both techniques simultaneously, an adaptive FEM/SPH approach can be employed. In this method, the local and adaptive transformation of Lagrangian solid elements to SPH particles is triggered by erosion of the solid elements when they become highly distorted and inefficient. The SPH particles replacing the eroded solid elements inherit all the nodal and integration point quantities of the original solids and initiated being attached to the neighbouring solid elements. LS-DYNA implementation of this technique was adopted in this study for the solution of two problems: (1) turbofan engine blade rub against the engine's fancase; (2) collision of an orbital debris particle with a sandwich panel of a spacecraft bus;. For the first problem, predictions of the adaptive technique are compared with those obtained using FEM-only and SPH-only models. For the second problem, a comparison of the numerical and experimental results is provided. The study highlights advantages and limitations of the adaptive modelling methodology.

2 MODELING TECHNIQUES

The three numerical schemes considered in this study were the finite element method, the smoothed particles hydrodynamics technique, and the adaptive FEM/SPH approach. All three methods are briefly described below.

Finite element method (FEM) combined with the element erosion. This approach usually provides a good balance between simulation accuracy and computational efficiency in impact problems; however, its applicability may vary depending on the levels of deformation experienced by elements in simulations. In addition, identifying erosion strain – a non-physical parameter determining the upper limit of deformation that an element can tolerate before removal from simulation – is often non-trivial.

Smoothed particle hydrodynamics (SPH) meshless technique, in which continuum is represented by the arbitrary lattice of interacting particles/interpolation points. This method eliminates mesh tangling problems inherent to the Lagrangian finite element method and does not require an erosion algorithm, which often makes it well suitable for high-speed impact

problems. The SPH method is, however, known to be more computationally expensive compared to FEM.

Adaptive (hybrid) FEM / SPH formulation (ADT), which allows finite elements to adaptively convert into meshless SPH particles at high deformation levels when the traditional finite element method becomes inefficient. In this method, the SPH particles replacing the failed solid Lagrangian elements inherit all the nodal and integration point quantities of the failed solid elements. Potential benefits of this technique, that required evaluation, are the reduced sensitivity to the erosion strain, as compared to the traditional FEM, and a possible reduction of computational time, compared to SPH.

3 CASE STUDY №1: FAN BLADE – ABRADABLE RUB STRIP INTERACTION IN TURBOFAN ENGINES

3.1 Background

Certification of an aircraft turbofan engine must demonstrate compliance with the bird ingestion, fan blade-off, and other high-speed impact requirements established by the airworthiness standards [1]. Engine manufacturers have made significant progress in creating high-fidelity numerical models for simulating the response of the engines to impact loading. In modeling, close attention is usually paid to simulating the interaction of fan blades with other parts of the engine. Such interactions may arise from deflection of the blades following a bird strike, ice shedding, or other events that may lead to rotor unbalance. This includes interaction of the blade with a lightweight potting compound that comprises the abradable rub strip (ARS) and has a function of minimizing the clearance between blade tips and the fan case. In the event of being hit by a foreign object, such as a bird entering the air intake of the engine, the blade may make a radial excursion coming into contact with the ARS. The microstructure of a generic abradable rub strip material is exemplified in Fig. 1. It comprises hollow glass microspheres randomly distributed in a polymer matrix, such as epoxy resin. Due to its composition, the material exhibits temperature softening (polymer matrix softens with temperature increase) and compaction under compressive loading (crushing of microspheres).

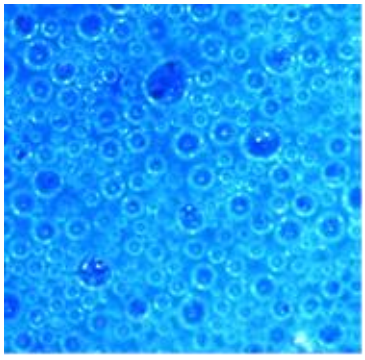

Figure 1: Microstructure of a generic abradable material comprising hollow glass microspheres randomly distributed in a polymer matrix

3.2 Numerical model

LS-DYNA's *EOS_TABULATED_COMPACTION was used in this study to quantify the significant volume changes that the material undergoes under compressive loading due to microspheres' crushing. Temperature effects on the strength of the material were accounted for in a simplified way. For blade rubs, the temperatures usually near or exceed the glass transition temperature of the polymer matrix of the rub strip material, leading to its plasticization and strength drop to "structurally insignificant" values. To capture this behavior in numerical simulations, the material was modeled as elastic-perfectly plastic using LS-DYNA's *MAT_ELASTIC_PLASTIC_HYDRO. For simplicity, the whole rub strip was assumed to be in the softened state, regardless of the vicinity of the material to the rub zone.

The simulation model used in this study to investigate the fan blade-ARS interaction is shown in Fig. 2. It includes models of a fan blade and of a 60° segment of the ARS attached to a flexible support (tray).

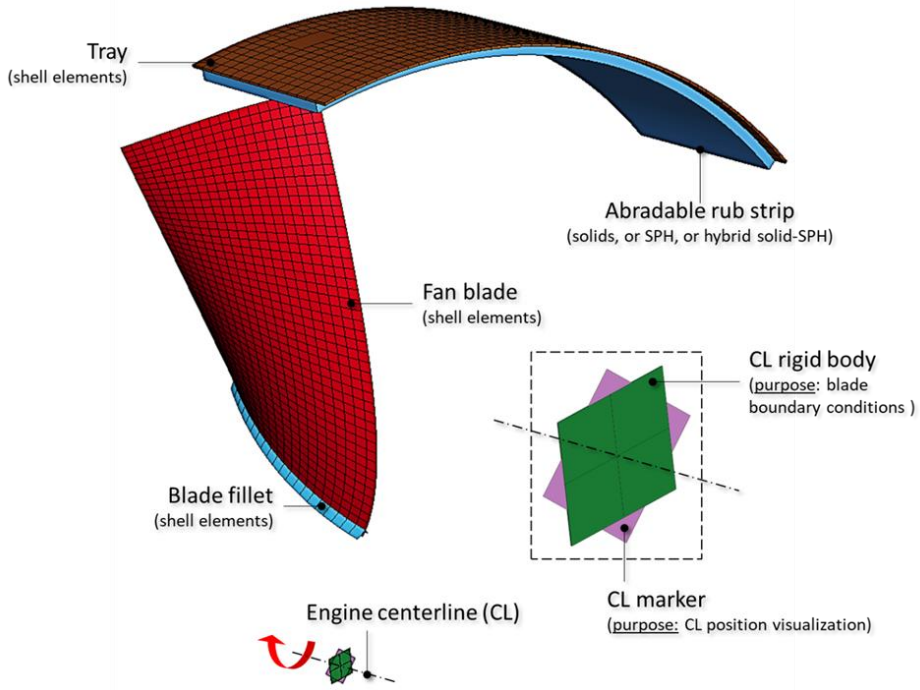

Figure 2: A generic simulation model for blade-abradable interaction studies

3.3 Metrics for the description of the blade–ARS interaction

The following metrics were used in this study to characterize the interaction of a fan blade with an abradable lining.

Morphology of the rub. Being qualitative, this metric encompasses any feature related to the shape of the damaged region formed in the abradable as a result of fan blade–ARS interaction. It also allowed distinguishing scenarios in which the damaged region represents a series of disconnected areas, as illustrated in Fig. 3. In this case, the first of such regions was referred to as a "primary rub", whereas all others were collectively referred to as "secondary rubs".

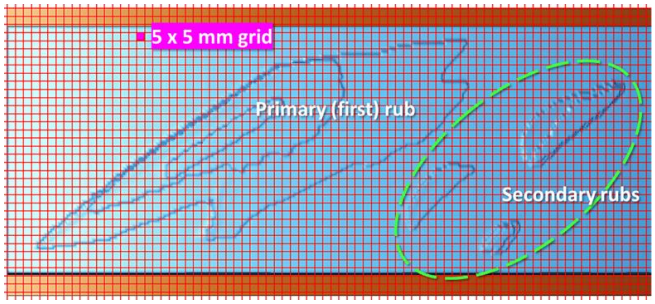

Figure 3: Damaged area calculation

Damaged area. This metric represents the projected area of the damaged region formed in the abradable as a result of fan blade-ARS interaction and calculated on the 5 mm x 5 mm grid, as shown in Fig. 3. If secondary rubs were present, the damaged area was calculated separately for the first rub and for the entire (total) damaged region that included both primary and secondary rubs. It should be emphasized that this metric represents only the two-dimensional projected area of the rub zone and does not quantify the volume of the damaged material.

Peak force. Represents a maximum resultant contact force during the first (primary) rub

seen on the contact force-time diagram, as shown in Fig. 4.

Process duration. A time interval corresponding to the duration of the first (primary) rub, as seen on the contact force-time diagram: $\Delta t=t_2-t_1$ (see Fig. 4).

Average force. Calculated as the area under the part of the force-time curve corresponding to the first (primary) rub, divided by the process duration.

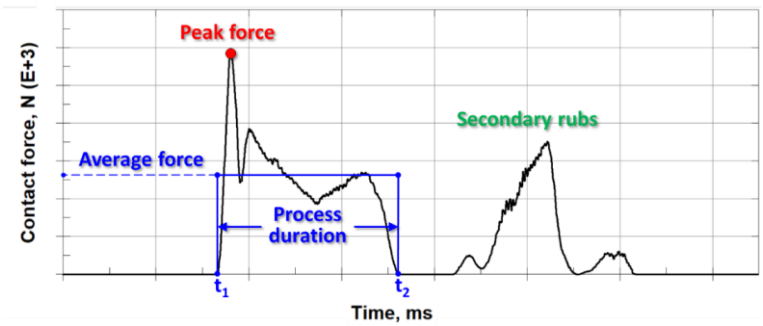

Figure 4: Peak force, average force, and process duration of the first rub

3.4 Mesh sensitivity

For the mesh sensitivity study, ARS was represented in the models using 3, 4, or 6 elements through the thickness. This corresponds to the element (or particle) size of 3.39 mm, 2.54, and 1.69 mm, respectively, such that the element size increment remains constant and equal to 0.85 mm.

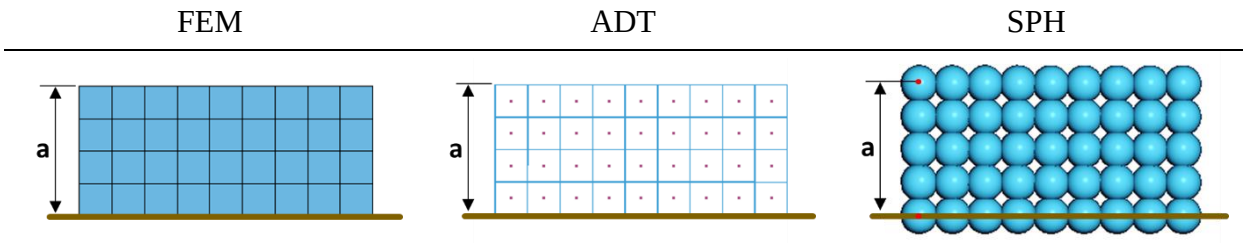

Figure 5: Abradable representation using the FEM, ADT, and SPH methods (the horizontal line defines the position of the tray; a – the thickness of ARS)

Discretization of a small segment of ARS using the three considered methods is shown in Fig. 5. and corresponds to the case of four elements through the thickness of ARS. For the adaptive technique, the SPH particles, that remain inactive until finite element erosion, are shown as dots inside solid elements. For SPH, as particles' centers are situated in the same positions as the nodes in the FEM and ADT models, the term "number of particles through-the-thickness" used in this study to describe SPH discretization of ARS, should be understood as "the number of particle diameters through-the-thickness".

All FEM and ADT models predicted notable secondary rubs, while in SPH models secondary rubs are negligibly small in terms of force and area. Morphology of the first rub also varies noticeably depending on the modeling technique and the density of discretization.

Peak force changed significantly with the change in the element size. This is especially the case for the FEM and ADT models, for which the variation of the peak force (the ratio of the standard deviation and the mean value for the given method) reaches ±44% (FEM) and ±28% (ADT) of its mean value. For the SPH models, the peak force varies by ±21%.

Similar trends are observed for the calculated average contact forces. The variation here is ±17% (FEM), ±28% (ADT), and ±10% (SPH) of the corresponding mean values. As it was with the peak force, the most consistent predictions of the average force with respect to the element size were obtained using the SPH model. This is also true for the duration of the first rub, which varied ±15% (FEM), ±28% (ADT), and ±6% (SPH).

Predictions of the damaged area were somewhat different for different methods; however,

for each numerical technique, the predicted area varied only moderately as a function of the element size. In particular, the prediction of the first rub damage varied ±14% (FEM), ±11% (ADT), and ±13% (SPH) of the corresponding mean values.

Depending on the mesh density and modeling technique, the computational time varied from 3.5 minutes to 3.5 hours. For instance, the 4 elements/particles SPH and ADT models consumed 64.98 and 58.10 min of machine time respectively, while the FEM model with 4 elements through the thickness of the ARS required only 5.98 minutes! It was therefore decided, in addition to the "equivalent element size" FE model, (EES; "equivalent" w.r.t. the other two methods – ADT and SPH), to introduce the "equivalent computational time" FE model (ECT), which would have a denser mesh and computational time of approximately 1 hour. It was determined that such a FEM model will have 10 elements through the thickness of the ARS (element size of 1.02 mm) and the run time of 58.67 minutes.

3.5 Sensitivity to erosion strain (a non-physical parameter)

Element erosion strain in the FEM and the ADT methods, is the artifact of the numerical scheme rather than physical property. It was therefore important to investigate its influence on the output of rub simulations.

The following observations were made. First, the morphology of the rub changed radically with the change of erosion strain. This also manifests itself in the change of the damaged area, which for the first rub varies as a function of erosion strain ±38% (EES FEM), ±25% (ECT FEM) and ±39% (ADT) of the corresponding mean values. Second, average rub force undergoes significant changes with the change of erosion strain, especially for the EES FEM (±25% of the mean) and the ADT (±32% of the mean) models. For the ECT FEM model, this variation is less pronounced and constitutes only ±13% of the corresponding mean value. Notably, estimates of the rub force obtained using the ECT FEM model are considerably lower than those calculated using the EES FEM and the ADT models. Finally, the choice of erosion strain will also affect the prediction of the process duration.

3.6 Sensitivity to incursion depth (a process parameter)

Additional simulations were conducted to investigate the response of the models to changes in incursion (rub) depth. Rub depths of 2.54 mm, 5.08 mm (default in the previously considered models), and 7.62 mm were considered. For the FEM and ADT models, the element erosion strain was kept constant and equal to 25%. Expectedly, the depth of incursion has a significant influence on the contact force, which tends to increase with the increase of the rub depth, as predicted by all models. However, the predictions have notable differences:

- Large spurious oscillations were noted on the F-t plots of the FEM EES and ADT models (4 elements through the ARS thickness). Such effects were not seen with the FEM ECT (10 elements through the thickness) and SPH (4 particles through-the-thickness) models.
- FEM (both EES and ECT) and ADT models predicted deep secondary rubs for all three considered incursion depth scenarios. Notably, predictions of the initiation of the secondary rubs, their duration, and force magnitudes were not consistent between the three models. In contrast, although secondary rubs were also predicted by the SPH model, their magnitudes were negligibly small compared to the primary (first) rub.
- The shapes/profiles of the F-t curves in the case of the 2.54 mm rub, as predicted by FEM (both EES and ECT) and ADT models, are notably different from those predicted for the

deeper rubs. In contrast, the SPH model predicted similar shapes for all three rub depths.

Calculated process metrics demonstrated the following:

- SPH model consistently predicted a linear or nearly-linear increase of all metrics with the increase of the rub depth. Such consistency is not seen with all other models.
- With the increase of incursion, the FEM ECT model predicts a notably non-linear change of the first rub damage and a linear change of the total damaged area. The opposite is true for the FEM EES model.
- The contact force predicted by the FEM ECT model is generally lower as compared to the predictions of the other models.
- Predictions of the total damaged area with all incursion depths are notably different for the SPH and the FEM ECT models.

3.7 Summary of observations for Case Study №1

The main features of the models developed using the three methods are summarized below.

- *FEM model*: strong mesh sensitivity of the results; a strong influence of element erosion strain on the results; fine meshes are required to reduce spurious oscillations of the blade, restricting the realization of the computational time benefit.
- *ADT model*: strong mesh sensitivity of the results; strong influence of element erosion strain on the results; increasing mesh density to reduce spurious oscillations of the blade may result in an enormous increase in computational time due to the presence of embedded SPH particles.
- *SPH model*: no sensitivity to non-physical parameters, such as erosion strain (not used with SPH); unlike the other models, predicted a consistent trend in change of all process metrics (rub force, process duration, damaged area) with the increase of the rub depth; no artificial excitation of the blade was observed.

4 CASE STUDY №2: ORBITAL DEBRIS IMPACT ON SPACECRAFT FOAM-CORE SANDWICH PANEL

4.1 Background

Sandwich panels are widely used in the design of unmanned satellites and in addition to having a structural function, can often serve as orbital debris shielding. In this application, sandwich panels with open-cell foam cores have a significant advantage, enabling intensive interaction between the impactor fragments and the foam ligaments which enhances the fragments' breakdown and reduces their damaging potential.

Figure 6: Open-cell aluminum foam – material used as a core in spacecraft sandwich panels

Assessing the orbital debris impact survivability of unmanned satellites requires the availability of predictive techniques and HVI simulation models for sandwich panels, which are capable of accounting for various impact conditions and design parameters. While complexity off the foam meso-structure usually requires its representation using a meshless method, such as SPH, other parts of the panel – its facesheets – can be modeled using the adaptive FEM/SPH technique.

4.2 Numerical model

A simulation model was developed to replicate the conditions of three physical experiments conducted by NASA using 1.0”-thick open cell foam core panels which were hit by 6.9 km/s aluminum projectiles. The experiments are denoted in Ref. [2] as follows: HITF 08261 (10 pores-per-inch [ppi] foam; 2.0 mm projectile); HITF 08253 (20 ppi foam; 2.0 mm projectile); HITF 08254 (20 ppi foam; 1.9 mm projectile). All panels included Al6061-T6 facesheets of 0.254 mm thickness, which were bonded to the core by (nominally) 0.241 mm-thick epoxy structural adhesive film. Different parts of the model are described below.

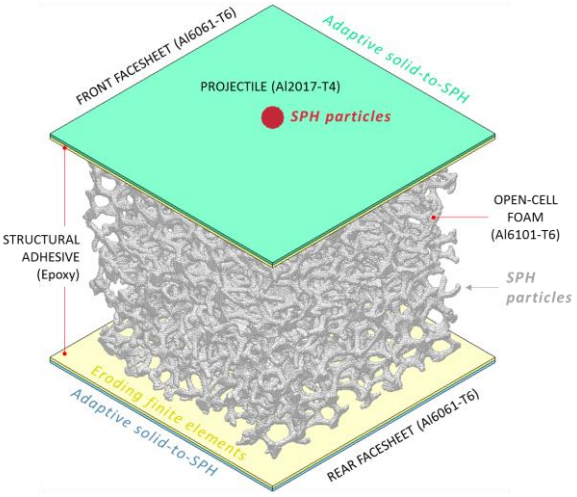

Figure 7: Hypervelocity impact simulation model of 1.0-inch-thick foam-core sandwich panel

Projectile. Due to the fact that a projectile, as a result of hypervelocity collision with a sandwich panel, was expected to experience fragmentation, SPH method was employed to represent this part of the simulation model.

Front facesheet was modeled using the adaptive FEM/SPH technique. This prevented numerical instabilities that could have happened if both facesheet and adhesive were modelled using SPH particles (significantly different densities) and allowed modelling of debonding between the facesheets and the adhesive.

Adhesive film was modelled using eroding Lagrangian finite elements without further conversion into meshless particles. Cohesive-zone modeling approach was used to simulate debonding between the facesheets and the adhesive layers that was observed experimentally.

Open-cell foam core was represented in the simulations explicitly using the SPH models derived from the CT-scan imaging of the real foam samples.

Rear facesheet. The ADT technique was employed for modelling of the rear facesheet. This approach made it possible to accurately capture different levels of rear wall damage: from small deformations (using solid elements) to very large deformations, converting distorted solid elements to SPH particles.

4.3 Results of simulations

Comparison of foam core damage – as predicted by the developed numerical model and obtained in NASA experiment HITF 08253 under the same impact conditions – is shown in Figure 8, from which it can be deduced that there is a good correlation between the numerical and experimental results in terms of the extent of the developed cavity in the foam.

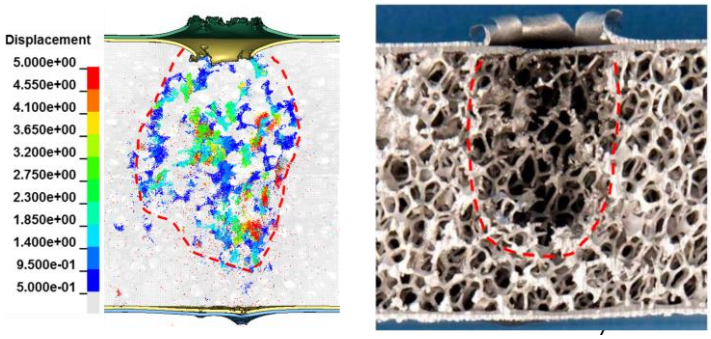

Figure 8: Impact damage of 20 ppi foam-core sandwich panel (model vs. experiment)

The main validation metric for the numerical model is its ability to accurately predict the ballistic limit

of a panel subjected to hypervelocity impact. The latter is usually linked to the rear facesheet damage resulting from the impact. For the three impact scenarios considered in this study, the corresponding modes of rear wall damage (close-up views with all parts other than rear wall hidden) are shown in Figure 9. They are represented by full perforation of the rear wall in the case of 2 mm projectile impacts (both cores), and no perforation in the case of the smaller 1.9 mm projectile impact on the sandwich panel with 20 ppi foam core. This is in line with the experimental observations reported by NASA (see Table 1).

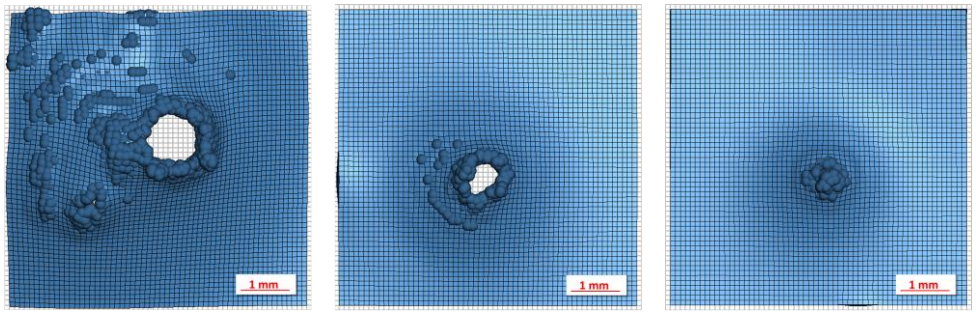

Figure 9: Rear facesheet damage as a function of projectile diameter and foam pore size

Table 1: Summary of simulations conducted to verify the developed numerical model and their correlation with available experimental data

#	NASA code	Target	Projectile, mm	Speed, km/s	Experiment (NASA)	Simulation (UWindsor)	D_{hole}, mm (experiment)	D_{hole}, mm (simulation)*
1	HITF 08261	1.0” Al F10	2.0	6.87	Perforation	Perforation	1.00	0.94
2	HITF 08253	1.0” Al F20	2.0	6.85	Perforation	Perforation	< 1	0.53
3	HITF 08254	1.0” Al F20	1.9	6.87	Pass	Pass	N/A	N/A

4.4 Summary of observations for Case Study №2

The simulation model developed in this study, featuring the explicit SPH-based representation of the open-cell foam core and the ADT-based modeling of the facesheets, demonstrated good correlation with the available experimental data in terms of its ability to predict the ballistic performance of foam-core sandwich panels subjected to impacts by hypervelocity projectiles.

5 CONCLUSIONS

The two problems considered in this paper demonstrate that efficiency of the adaptive modeling in high-velocity impact simulations may vary significantly depending on the problem being solved. As can be deduced from the first case study, it is important for an analyst to consider alternative options when possible. The second case study demonstrates that the adaptive method can be efficiently used in combination with other modeling techniques within the same simulation framework.

REFERENCES

[1] Code of Federal Regulations, title 14, part 33. Airworthiness Standards: Aircraft Engines.
[2] Ryan S., Christiansen E. Hypervelocity impact testing of aluminum foam core sandwich panels. NASA/TM–2015–218593.